Fish can save energy via proprioceptive sensing

Bioinspiration & Biomimetics

OPEN ACCESS

PAPER

Fish can save energy via proprioceptive sensing

Liang Li[1,2,3,*], Danshi Liu[4], Jian Deng[4,*], Matthew J Lutz[1,2,3] and Guangming Xie[5,6]

[1] Department of Collective Behaviour, Max Planck Institute of Animal Behavior, Radolfzell am Bodensee 78315, Germany
[2] Centre for the Advanced Study of Collective Behaviour, University of Konstanz, Konstanz 78464, Germany
[3] Department of Biology, University of Konstanz, Konstanz 78464, Germany
[4] Department of Mechanics, Zhejiang University, Hangzhou 310027, People's Republic of China
[5] State Key Laboratory for Turbulence and Complex Systems, College of Engineering, Peking University, Beijing 100871, People's Republic of China
[6] Institute of Ocean Research, Peking University, Beijing 100871, People's Republic of China
[*] Authors to whom any correspondence should be addressed.

E-mail: lli@ab.mpg.de and zjudengjian@zju.edu.cn

Keywords: schooling fish, robotic fish, proprioceptive sensing, hydrodynamic interaction, energy saving

RECEIVED
29 May 2021

REVISED
12 July 2021

ACCEPTED FOR PUBLICATION
20 July 2021

PUBLISHED
16 August 2021

Abstract

Fish have evolved diverse and robust locomotive strategies to swim efficiently in complex fluid environments. However, we know little, if anything, about how these strategies can be achieved. Although most studies suggest that fish rely on the lateral line system to sense local flow and optimise body undulation, recent work has shown that fish are still able to gain benefits from the local flow even with the lateral line impaired. In this paper, we hypothesise that fish can save energy by extracting vortices shed from their neighbours using only simple proprioceptive sensing with the caudal fin. We tested this hypothesis on both computational and robotic fish by synthesising a central pattern generator (CPG) with feedback, proprioceptive sensing, and reinforcement learning. The CPG controller adjusts the body undulation after receiving feedback from the proprioceptive sensing signal, decoded via reinforcement learning. In our study, we consider potential proprioceptive sensing inputs to consist of low-dimensional signals (e.g. perceived forces) detected from the flow. With simulations on a computational robot and experiments on a robotic fish swimming in unknown dynamic flows, we show that the simple proprioceptive sensing is sufficient to optimise the body undulation to save energy, without any input from the lateral line. Our results reveal a new sensory-motor mechanism in schooling fish and shed new light on the strategy of control for robotic fish swimming in complex flows with high efficiency.

1. Introduction

Fish live in complex fluid environments, and have evolved various sensory-motor strategies to improve swimming efficiency [1]. For example, when swimming in Kármán vortices, rainbow trout switch to the Kármán gait to extract energy from the fluid environment [2]. Schooling fish are able to dynamically optimise body undulations to save energy and thus improve swimming efficiency, regardless of their spatial formations [3, 4]. Although we know schooling fish benefit from hydrodynamic interactions, the mechanisms by which they achieve these gains are not well understood.

Vision [5] and lateral line [6] are two main sensory modalities used by fish to collect environmental information and make movement decisions. However, several studies have shown that fish can still react to their nearby flows when the lateral line and/or vision systems are impaired [4, 7]. Here, we hypothesise that fish can also use proprioception to sense the local flow dynamics, and thus to adjust kinematics to save energy [8, 9]. The term proprioception was first used by Sherrington [10], includes both self-motion-sensing and muscle force sensing [11]. This sensory system has been widely studied in tetrapods [12] and even in the human body [11, 13]. Proprioceptive sensing is also found in fish, and it has been shown that fish can use this modality to sense flow information as well [14–16].

In addition to a sensor, fish also require a locomotion controller to save energy when schooling. The main locomotion controller in most animals is known as a central pattern generator (CPG) [17–19], which is a neural network that produces rhythmic signals while receiving simple brain-level control. Although

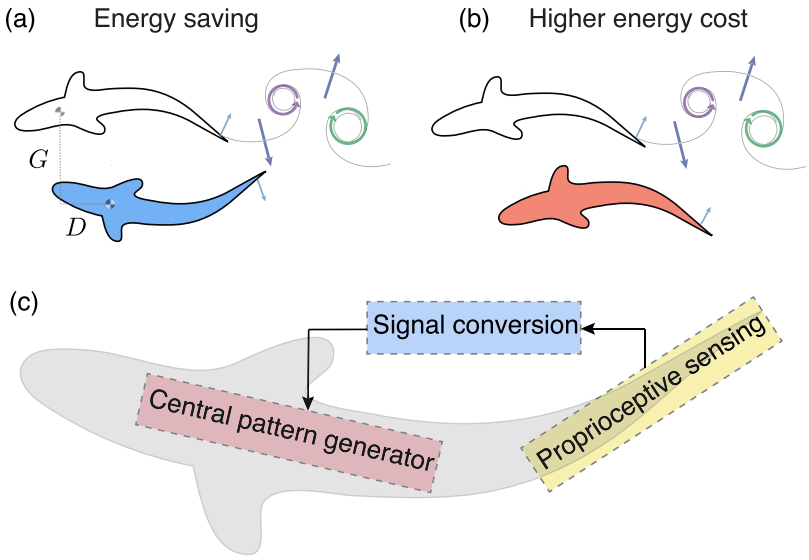

Figure 1. Schematic of the proprioceptive sensing feedback hypothesis. (a) and (b) The follower interacting with the same flow fields can save energy (a) or cost more energy (b) due to different body undulations. In this case, the flow fields are determined by front–back distance, D, left–right distance, G, and specific body phase, Φ (see definition in figure 2). (c) The proprioceptive sensing signals are used as a feedback to the CPG.

sensory feedbacks are not necessary to generate rhythmic signals, they play an important role in shaping the CPG control [17, 18]. In this paper, we consider the proprioceptive sensing as the sensory feedback for the CPG controller [11].

Whether, and if so, how real fish may use proprioceptive sensing to optimise the CPG controller to save energy when schooling remains an open question. However, this hypothesis is difficult to test experimentally with live fish, because impairment of the proprioceptive system may also impair the motor system. In this paper, we test this hypothesis with both a computational model and experiments with a bio-inspired robotic fish, swimming in complex neighbour-induced flow vortices. The upstream neighbour (leader) randomly changes its kinematics to generate unsteady flows, which is unknown to the focal individual. Both computational and robotic fish optimise their body undulations based on the proprioceptive sensing, decoded by reinforcement learning and further transferred to the CPG controller. We explore and compare the energy cost of fish swimming in dynamic flows with and without (random body undulation) proprioceptive sensory feedback. Both simulations and experiments show that fish can save energy via simple proprioceptive sensing and the CPG controller with feedback.

The main contributions of this article include: (1) we propose a hypothesis that schooling fish can save energy purely based on the proprioceptive sensing. (2) To test this hypothesis, a simple framework is developed, which combines CPG with feedback and reinforcement learning. (3) Both numerical simulations and robotic fish experiments are carried out, demonstrating that both the simulated fish and the robotic fish can explore low-cost undulation by using only the proprioceptive sensing.

2. The proprioceptive sensing hypothesis

We hypothesise that fish can optimise body undulation, which is controlled by a CPG, relying only on proprioceptive sensing. To test this, we consider a simplest case where two fish swim in a constant incoming flow (or equivalently at a constant swimming speed) and a fixed spatial arrangement, i.e. fixed front–back and left–right distances, D and G, as shown in figure 1(a). Similar to the natural environment, neighbours induce complex fluid flows, which are usually unpredictable to the focal individual. According to our previous study [4], with two fish swimming in a stable formation, the follower can adjust its body undulation relative to the leader to achieve different levels of energy consumption (see figures 1(a) and (b)). To achieve this, fish need to first sense the flow environment and then control their locomotion based on feedback from the flow sensor (see figure 1(c) for the schematic). A 'signal conversion' block receives the proprioceptive sensing signal and decodes the signal to drive the CPG controller. We propose reinforcement learning as the signal conversion since the neurotransmission mechanism is unknown.

2.1. The body phase

Previous studies [4, 20] have shown that a follower can save energy by adopting an optimal body undulation relative to a leader, depending on their spatial configurations (see figures 1(a) and (b)). Therefore, fish is able to save energy purely by adjusting the body

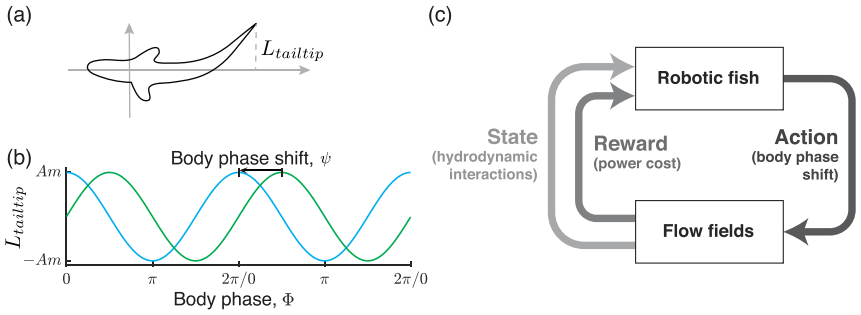

Figure 2. Schematics of the test procedure for proprioceptive sensing feedback. (a) and (b) show the definitions of body phase, Φ, and the body phase shift, ψ, respectively at a certain time instant. (c) The signal conversion is achieved by reinforcement learning.

undulation, or specifically the body phase, Φ, according to the lateral displacement of the tail tip. As the tail tip flaps to its maximum positive lateral position (shown schematically in figure 2(a)), the body phase, Φ is $\pi/2$, and this varies from $0 \sim 2\pi$ as the tail tip oscillates in one period (figure 2(b)).

In this paper we have introduced a shift, ψ, to the body phase in equation (2), by which we can actually modify the undulation. In order to further explain this, we use a simplified undulating equation, with varied and increasing amplitude from the nose to the tail tip, to represent the fish locomotion.

$$z(s,t) = (c_1 s + c_2 s^2)\mathbf{sin}(2\pi ks/L + \omega t), \qquad (1)$$

where $z(s,t)$ denotes the lateral displacement of each discrete points on the fish, and s is the tangent component of the natural coordinate along the central line of the fish, which varies from 0, the nose, to L, the tail tip, where L is the length of the fish. In the current study, we set $k = 0.24$. In equation (1), c_1 and c_2 are linear and quadratic components of the wave amplitude, and ω is the angular frequency. Adding a body phase shift ψ to equation (1), we get

$$z(s,t) = (c_1 s + c_2 s^2)\mathbf{sin}(2\pi ks/L + \omega t + \psi). \qquad (2)$$

The leader and the follower can take different phase shifts ψ, resulting in a phase difference (PD) $\psi_1 - \psi_2$.

Figure 2(b) shows a modified undulation with a phase shift of $\psi = \pi/2$ ahead of its original formulation. Therefore, in these terms, the follower can switch between the states shown in figures 2(a) and (b) with $\psi = \pi/2$. To generate unsteady and random ambient flows for the follower, we randomise the leader's body phase shift at regular intervals. In such a scenario, the follower needs to adjust dynamically its body phase shift to save energy. We should note that instead of the individual body phase Φ of each fish, we concern more with their difference, or equivalently the difference in their body phase shift ψ.

2.2. Reinforcement learning for conversion of proprioceptive sensing signal

Since the muscle spindles have been shown to function in a number of animals as receptors that can be used to sense forces while moving [11, 13], here we mainly consider the force or force-related signals as the proprioceptive signal from the caudal fin. For example, in figures 1(a) and (b), the caudal fin perceives different forces along the tail depending on the direction of its movement due to different hydrodynamic interactions.

A mechanism of information transfer is required to send the sensory signal as feedback to the CPG controller. In animals, this occurs via neural network, for example, a fish may transfer the bending of its fin to a specific neural signal as a stimulus for body movement. Since we do not know the neurotransmission mechanism between proprioceptive sensing and locomotion control, here we apply a simple reinforcement learning algorithm to transfer the measured proprioceptive signal to a neural, or control, signal. Reinforcement learning enables agents to find the optimal action by trial-and-error interactions with the environment, and has been widely applied in the field of robotics [21, 22].

We applied a Q-learning algorithm [22, 23] to decode the proprioceptive signal to the body phase shift ψ. Figure 2(c) shows a schematic of reinforcement learning. The follower has its body phase shift ψ as the 'action', hydrodynamic interactions as the 'state', and energy cost as the 'reward'. The robotic fish learns through trial-and-error interactions with the flow environment, with the goal of maximising energy savings. A Q-table is designed to assess this value as a function of state and action, and is updated according to

$$Q(s,a) = Q(s,a) + Q_\alpha \left[Q_r + Q_\gamma \max_{a'} Q(s',a') - Q(s,a)\right], \qquad (3)$$

where s is the state vector, a is the action vector; $Q(s,a)$ is the evaluated value of the performing action a in the state s; Q_r is the immediate reward of the current action; Q_α is the learning rate and Q_γ is the discount factor. s' denotes the next state, $\max_{a'} Q(s',a')$ predicts the optimal future reward based on the optimal action (a') for the next state. Therefore, the Q value evaluates the actions in each state in a global view.

Actions: we consider the discrete body phase shift ψ as an action, with previous studies have shown to be effective towards achieving the goal of minimising energetic costs [4]. **Reward:** we measure the power cost of the computational and robotic fish as the immediate reward of the current action and state. Because of the noise in computational fluid dynamics (CFD) and experiments, one may get different reward values at the same action and state but at different time. **State:** the state is given by estimation of the nearby flow environment via proprioceptive sensing, based on various forces in the simulations and the power costs measured in the experiments. **ϵ-greedy policy:** we used a simple ϵ-greedy policy for the exploration of potential body phases in dynamic fluid environments. The robot adopts an action with a 1-ϵ probability that gives a maximum long-term reward. Otherwise, the robot chooses an action uniformly from the collection of actions at random. $0 < \epsilon < 1$ balances exploration and exploitation, with larger ϵ values indicating more exploration.

2.3. CPG with feedback

Inspired by the biological system, where the CPG may determine the initial body phase and update this according to the proprioceptive sensory feedback [13], we developed a CPG controller based on the framework described in our previous study [24], modified with a feedback loop that adjusts the body phase shift ψ of the robotic fish. The oscillation of each joint can be described by the following model:

$$\dot{r}_i(t) = \alpha(R_i - r_i) \tag{4}$$

$$\dot{x}_i(t) = \beta(X_i - x_i) \tag{5}$$

$$\dot{\psi}_k(t) = \gamma(\Psi_k - \psi_k) \tag{6}$$

$$\ddot{\phi}_i(t) = \sum_{j=1, j\neq i}^{N} \mu\left[\mu\left(\phi_j(t) - \phi_i(t) - \varphi_{ij}\right) - 2\left(\dot{\phi}_i(t) - 2\pi\omega\right)\right] \tag{7}$$

$$\theta_i(t) = x_i(t) + r_i(t)\sin(\phi_i(t) + \psi_k), \tag{8}$$

where r_i, x_i, and ϕ_i respectively denote the amplitude, offset, and phase, respectively, of the ith oscillator, and R_i, X_i, φ_{ij}, and ω are the locomotion control parameters, representing the amplitude, offset, phase difference between two joints and frequency, respectively. θ_i is the output angle for each joint of the robot. ψ_k represents the body phase shift of the kth robot. Ψ_k is the desired body phase shift of the kth robot, as decoded from sensory feedback, such as the lateral line, vision or proprioceptive sensors. α, β and γ are structural parameters, which indicate how fast the system converges to the preset values. In equations (4)–(8), i denotes the different joints, while k denotes the different robotic fish. We have to point out that the fish's locomotion is actually realised by using the CPG controller through these equations, instead of equation (2). However, in some sense, we can say that the CPG controller is a discretised realisation of equation (2) [25].

Equations (4) and (5) describe the dynamic convergence of the amplitude and offset, when the control of the amplitude and offset change. The dynamic convergence of the feedback signal is the desired body phase shift, Ψ_k. Equation (6) illustrates how the body phase dynamically converges to the desired body phase value, which is decoded based on the proprioceptive sensory feedback. Equation (7) describes the dynamic phase control of the frequencies and phase differences between each of the two joints. Equation (8) denotes the output of the angle of each joint to form the undulation pattern according to the parameter setting.

We first verified the effectiveness of the feedback CPG controller with a test simulation by numerically solving equations (4)–(8), described as follows: two fish (fish 1 and fish 2) swim at a fixed distance apart, starting with a body phase difference of 0 ($\psi_1 - \psi_2 = 0$), as shown in figure 3. After 4 s, the body phase of fish 1 was shifted with π phase lead, converging to the desired body phase shift within one period (figure 3). As expected, the resulting body phase difference between the two was $\psi = \pi$, and the test simulation verified that the body phase shift occurred smoothly, which protects the robotic fish motors from overload.

3. Results

3.1. CFD simulations

We first conducted 2D CFD simulations to test our hypothesis. For simplicity, we modelled the fish body as a one-dimensional filament with three joints, spaced with the same ratio as in the robotic fish. The Reynolds number is around 2000. Locomotion was also controlled by the CPG controller (see table 1 for the parameters). Since we do not know which force the fish would take as the proprioceptive sensing signals, we tested different force components of the perceived resultant force vector. They are lateral force (f_x), longitudinal force (f_y), resultant force (f_x, f_y) and frictional force (f_c) (see figure 4).

We developed a custom code based on the finite-volume method to numerically solve the time-dependent, incompressible form of the Navier–Stokes equation [26]. The differential form of the momentum equation for a viscous, incompressible fluid is

$$\rho\left(\frac{\partial \mathbf{u}}{\partial t} + \mathbf{u}\cdot\nabla\mathbf{u}\right) = -\nabla p + \mu\nabla^2\mathbf{u} + \mathbf{f},$$
$$\nabla\cdot\mathbf{u} = 0, \tag{9}$$

where $\rho, \mathbf{u}, p$ are the density, velocity and pressure of the fluid, respectively. An extra forcing term $\mathbf{f}$ is included to represent the fish body immersed in the

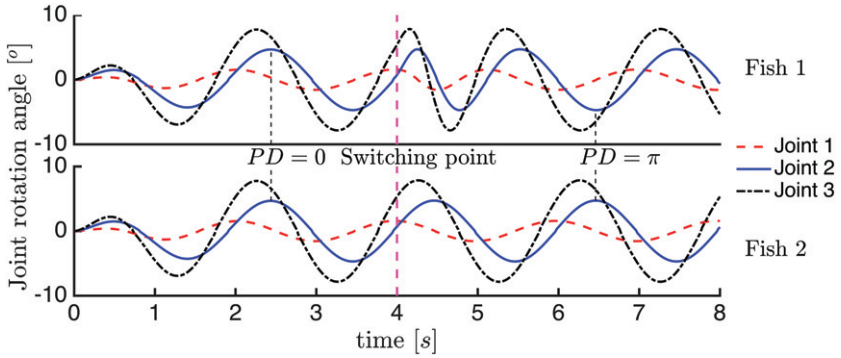

Figure 3. Example of body phase control. Two fish (fish 1 and fish 2) swim together with various body phase differences PDs (PD $= \Psi_1 - \Psi_2$ body phase of fish 1 Ψ_1 minus body phase of fish 2 Ψ_2). For the first 4 s, two fish swim with the same body phase (PD $= 0$); fish 1 shifted its body phase at $t = 4$ s with body phase lead of π. With our control algorithm, the two robotic fish switched their body PD from 0 to π smoothly.

Table 1. Parameters for CPG controller.

Parameter	Value	Unit
R_1	12	degree
R_2	22	degree
R_3	26	degree
X_1	0	degree
X_2	0	degree
X_3	0	degree
φ_{12}	1.396	rad
φ_{13}	2.094	rad
ω	0.85	rad s^{-1}

fluid flow, calculated using the so-called immersed boundary method [27], by the integration of the Lagrangian forcing density $\mathbf{F}(s,t)$ on the fish weighted by a Dirac delta function, as

$$\mathbf{f}(\mathbf{x},t) = \int \mathbf{F}(s,t)\delta(\mathbf{x} - \mathbf{X}(s,t))\mathrm{d}s, \qquad (10)$$

where $\mathbf{x}$ is fixed Cartesian coordinate, t is the time and s labels a fixed material point in Lagrangian form. The Dirac delta function in its discrete form is expressed as

$$\delta_h(\mathbf{X}) = h^{-2}\zeta(\frac{X}{h})\zeta(\frac{Y}{h}), \qquad (11)$$

where h is the length of the computational cell, X and Y indicate the position of the computational cell, and ζ function is defined as

$$\zeta(q) = \begin{cases} \dfrac{3 - 2|q| + \sqrt{1 + 4|q| - 4q^2}}{8} & \text{if } |q| \leqslant 1; \\ \dfrac{5 - 2|q| - \sqrt{-7 + 12|q| - 4q^2}}{8} & \text{if } 1 < |q| < 2; \\ 0 & \text{if } |q| \geqslant 2. \end{cases} \qquad (12)$$

For a fish with prescribed motion, the Lagrangian forcing density $\mathbf{F}$, imposed by the fluid on the fish and can be computed as

$$\mathbf{F} = \alpha \int_0^t (\boldsymbol{U}_{ib} - \boldsymbol{U})\,\mathrm{d}t' + \beta\,(\boldsymbol{U}_{ib} - \boldsymbol{U}), \qquad (13)$$

where $\boldsymbol{U}_{ib}$ is the interpolated fluid velocity on the fish, $\boldsymbol{U}$ is the velocity of the fish, and α and β are negative constants. More details of the numerical implementation can be found in our previous study [28, 29].

By integrating $\mathbf{F}$ along the fish, we can obtain the perceived resultant force vector (f_x, f_y), with its lateral and longitudinal components written respectively as

$$f_x(t) = \int \mathrm{F_x}(s,t)\mathrm{d}s \quad \text{and} \quad f_y(t) = \int \mathrm{F_y}(s,t)\mathrm{d}s. \qquad (14)$$

The frictional force can be calculated by

$$f_c(t) = \int F(s,t) \cdot \mathrm{d}\mathbf{s}, \qquad (15)$$

and the power cost is estimated by

$$P = \int -\mathbf{F}(s,t) \cdot \boldsymbol{U}\,\mathrm{d}s. \qquad (16)$$

Two fish were simulated swimming in a stable staggered formation ($D = G = 0.31$ L) with the incoming flow at a speed of 0.62 L s^{-1}. To carry out a mesh independence study for the numerical model, we first set the body phase shifts to zero. In the x-axis (along the fish body) and y-axis (perpendicular to the fish body), the mesh cells were uniformly distributed. We studied the longitudinal forces f_x on different mesh resolutions, with $\triangle x$ and $\triangle y$ varying from $L/20$ to $L/200$. We found that the medium

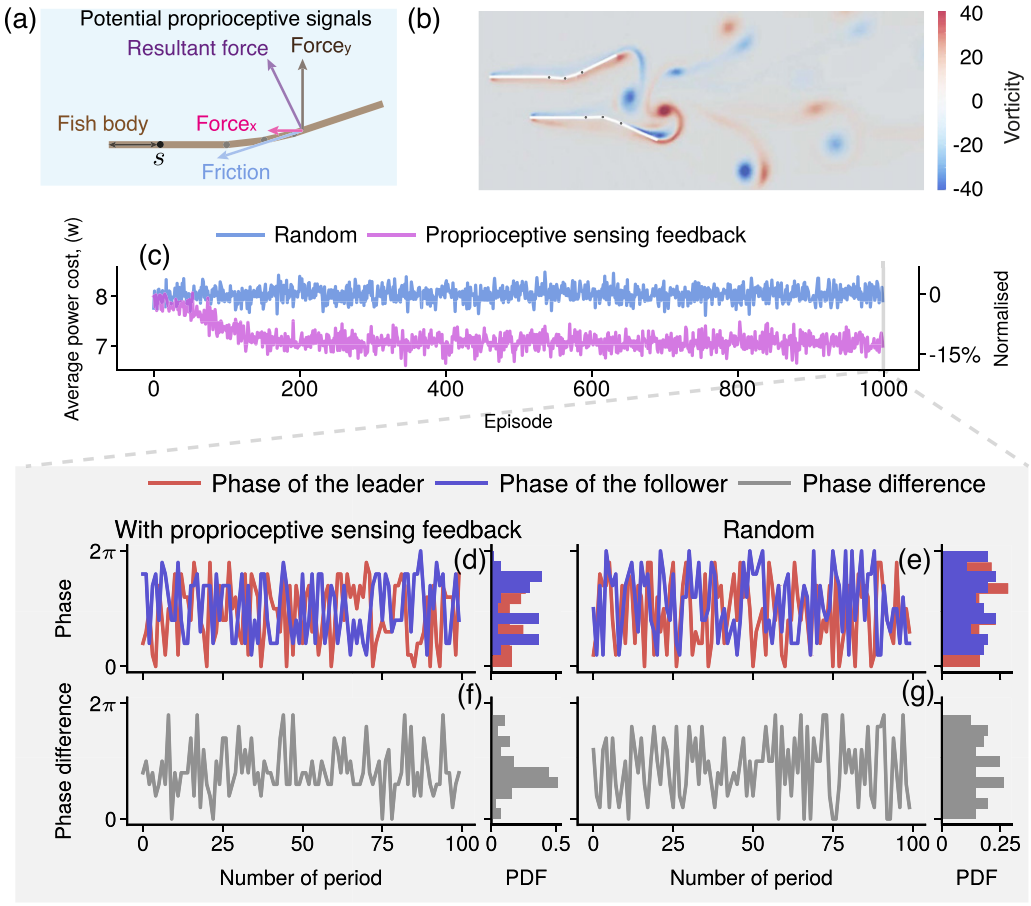

Figure 4. Verifying the hypothesis via CFD. (a) Schematics of the force components as perceived proprioceptive sensing signals. (b) Flow fields generated by two simulated fish swimming in stable formation. (c) The power cost of the follower over 1000 simulated episodes, with and without proprioceptive sensing (here with the friction as the sensing signals, while those with other force components are shown in figure 5). The relative energy saving, normalised by the average power cost of randomised strategies, is shown by the vertical axis labels at the right side of (c). (d)–(g) For one (final) episode: phases of leader and follower (d), (e), and PD (f), (g), with (d), (f) and without (e), (g) proprioceptive sensing feedback.

mesh with $\triangle x = \triangle y = L/80$ was sufficient to achieve satisfactory results. The total number of mesh cells was 76 800, and the time step size was $\triangle t = 0.001$. By compromising between efficiency and accuracy, we used this medium mesh for our following numerical simulations.

For the controlled fish, the leader was given ten discrete values for its body phase (Ψ_{Leader}), ranging from 0 to 2π at an interval of 0.2π, with each phase held for 5 s (proprioceptive sensing is based on the last one period 1.176 s). The simulated flow environments were designed with a random sequence of these discrete values. The simulated leader fish generated the dynamic fluid for the follower with follower with 100 random body phase shifts Ψ_{Leader} (theoretically, this can be an arbitrary number).

In our test simulations, the follower was allowed to optimise its body phase shift (Ψ_{Follower}) to maximally save power cost over each episode (averaged over one period of body undulation), based on reinforcement learning according to the algorithm above, with simulated sensory input from one of four potential proprioceptive forces. For each of the four forces, we ran a total of 1000 simulated episodes (defined as the follower swimming through all 100 of the dynamic fluid states from the leader's phase shifts) with $Q_\alpha = 0.01$ and $Q_\gamma = 0.4$. Another set of 1000 episodes, in which the follower adopted random body phase shifts, were simulated as a control, for comparison.

For all four potential forces tested, after around 200 episodes, the simulated follower reached a stable state of significant power reduction, as shown in figure 4(c). Detailed body phases of the leader and follower, and phase differences with and without proprioceptive sensing in the last episode are shown in figures 4(d)–(g). With proprioceptive sensing, the follower converged to a typical phase difference, indicating the targeting of constructive hydrodynamic interactions based solely on proprioceptive sensing feedback. For clarity, simulation results using just one of the potential forces (friction) as the proprioceptive sensing signal are shown in figures 4(c)–(g). However, we found that all four potential perceived forces were similarly effective for proprioceptive sensing feedback, as shown in figure 5.

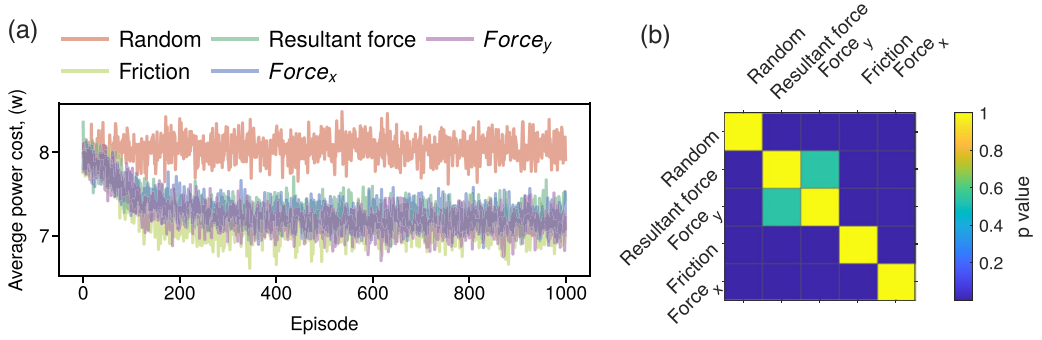

Figure 5. Testing different force components as the proprioceptive sensing signals for locomotion control. (a) Estimated power costs for different force signals, comparing to random body phase shifts. Here, the resultant force means the force magnitude. (b) Differences measured by ANOVA (analysis of variance) for the five different cases.

3.2. Experiments with robotic fish

Next, we tested the hypothesis with two robotic fish, a leader and a follower, swimming in fixed formation in a flow tank (figures 6(a) and (b)). The robotic fish is 45 cm in length and 800 g in mass; the aspect ratio of the tail is 2.4 [30]. As in the simulation, the leader controlled the flow environment by randomly shifting its body phase (control Ψ_{Leader}), and the follower tried to reduce its energy consumption by shifting its body phase (only update Ψ_{Follower}). Experiments were carried out in a flow tank 40 cm wide and 45 cm deep, with free stream turbulence less than 0.5%, at the College of Engineering, Peking University [31]. Two robotic fish were fixed in the middle layer of the water to reduce the effects of the boundaries (figure 6(b)). The CPG control parameters (see table 1) were chosen based on our previous studies with robotic fish and CFD simulations [4, 24, 25]. The flow speed $u = 0.278$ m s^{-1}, corresponding to the Reynolds number around 10^5, was set according to the free-swimming speed of the robotic fish with the same CPG parameters. The robotic fish were positioned at the same left–right distance G and front–back distance D ($G = D = 0.14$ m), which we previously determined to be an effective formation for interacting [4].

The power consumption was evaluated with a DC (direct current) stabilised power supply (DP 832) and a current acquisition module (National Instruments, NI 9227) set to a rate of 5000 sample/s to reduce the effects of noise. The power for the robotic fish was set to 6.2 ± 0.1 V. The power cost (in watts) is the product of the voltage and current. Since the power cost of the follower is directly linked to the perceived force of the body, we consider the power cost as a proxy estimate for the perceived proprioceptive signal. To reduce the deviation of the power detection, we use the average power cost over one period instead of instantaneous values.

At first, we generated 100 random body phase shifts Ψ to produce different discrete reverse Kármán vortices fluid environments, as in the simulations, and defined one episode as the follower swimming through all of these. The follower swam in a stable formation to optimise its body phase shift, ψ, to save maximum energy. The follower detected and averaged the energy consumption of every undulation period. The average value (immediate reward Q_r) and current action ($a = \Psi$) were then transferred to the Q-learning algorithm as the reward and to estimate the state. In total, we ran the experiment for 300 episodes with $Q_\alpha = 0.1$ and $Q_{\text{gamma}} = 0.2$. As a control for comparison, we also ran experiments in which the follower swam with random body phase undulations.

As shown in figure 6(c), after around 50 episodes, the power cost of the follower employing the learned proprioceptive sensing began to reduce, converging to a stable state after around 100 episodes. Comparing power consumption in this stable state (over the last 100 episodes), the robotic fish with proprioceptive sensing, using Q-learning, used significantly less power in watts (mean = 2.7621, SD = 0.0040) than the random phase shifting control (mean = 2.8013, SD = 0.0045), t (200) = 65.69, $p < 0.001$. The respective phases of the two fish during the last episode are shown in figures 6(d) and (e). Comparing the phase differences with and without feedback control (figures 6(f) and (g)) shows the follower with proprioceptive sensing converged to a typical phase difference, thus achieving power cost savings. This result indicates that the follower was able to maintain the constructive hydrodynamic interaction using simple proprioceptive sensing.

4. Discussion and conclusion

In this paper, we tested the hypothesis that fish can save energy by using proprioceptive sensing while swimming in complex fluid environments. Using CFD simulations and experiments with robotic fish in a flow tank, we found that both simulated and robotic fish were able to optimise body undulations relative to a leader fish to save energy. In both cases, this was accomplished via our model of proprioceptive sensing. We implemented a CPG controller

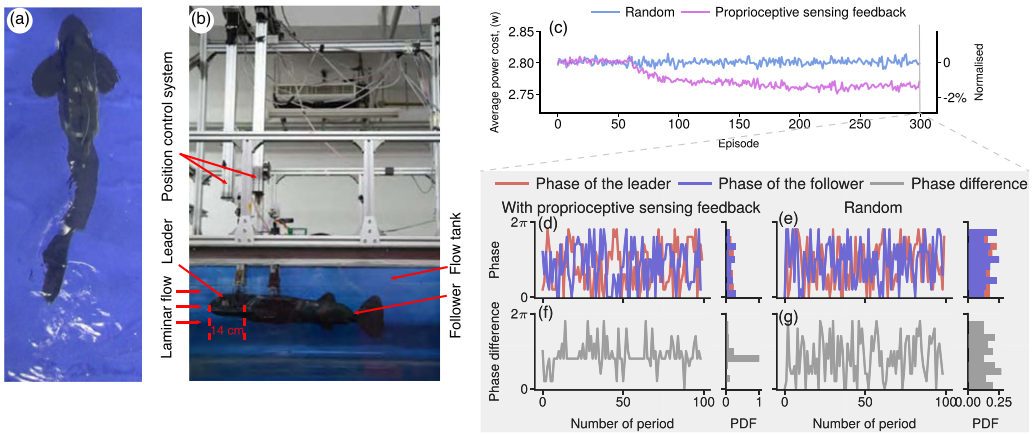

Figure 6. Robotic fish experiments to verify the hypothesis. (a) The robotic fish model used in the experiments. (b) The setup for the test. (c) Power costs of the follower swimming with and without proprioceptive sensing in 300 episodes. The relative energy saving, normalised by the average power cost of randomised strategies, is shown by the vertical axis labels at the right side of (c). (d)–(g) Phases of leader and follower ((d), (e)), and PD ((f), (g)) in the last episode: with ((d), (f)) and without ((e), (g)) proprioceptive sensing feedback.

with feedback to control body undulation according to proprioceptive sensing, and applied a Q-learning algorithm to decode the proprioceptive signals for feedback into the CPG. Our results show that follower fish were capable of sensing and taking advantage of local hydrodynamic forces generated by leader fish, solely using the mechanism of proprioceptive sensory feedback. This indicates that real fish may also be able to sense local flow by this modality, without inputs from the lateral line or vision.

We measured the power consumption of the robotic fish directly, considering this a proxy estimate for the energetic costs of swimming. Comparing the energy consumption of a robotic fish swimming in unpredictable dynamic fluid environments with and without proprioceptive sensory feedback, we found that the robot was able to save energy, relying solely on proprioception. Our results are consistent with previous studies showing that the fish fin itself may be capable of detecting the flow environment [14, 15, 32]. The lateral line is useful for detecting flow near the head of a fish [33], while the muscle spindle is useful for sensing the flow environment near the body and tail. There are many possibilities regarding what may constitute the perceived proprioceptive signals, such as forces perceived by the fish body, or the power cost of body undulation. Identifying exactly which of these are important for various fish species, and under what conditions, remains an important task for future work. Our results, showing the likelihood of proprioceptive sensing in fish should provide a basis for such investigations, with our CFD framework enabling theoretical exploration of these potential forces.

In both the numerical simulations and the robotic fish experiments, we found that the converged body phase differences are around π, the anti-phase, which is consistent with the optimal phase difference (resulting in maximum energy saving for the follower) found previously between the two robotic fish swimming at a similar configuration [4]. Therefore, the energy saving can be attributed to the same physical mechanism, vortex-phase matching, in the way that the follower tunes its tail undulation according to the reverse Kármán vortices in the wake of the leader. We also note that the energy saving in 2D numerical simulations is larger than that of the 3D experiments, due to the simplification of our numerical model [4].

The CPG controller implemented here not only controls the phase differences between each two joints for every individual, but can also manipulate the body phase differences between multiple individuals. This should prove useful for further studies with multiple robots incorporating spatial formation and body phase control, since real fish do modify both of these when swimming in groups [4, 34]. In an applied context, this work could also inform future energy-saving designs for autonomous underwater vehicles.

Our study offers a feasible explanation for the long-standing question of how fish with impaired visual and lateral line sensing are still able to interact with nearby flows [4, 7]. The setup employed here, with two robotic fish swimming in a flow tank, in a fixed formation and with one-dimensional action (the body phase shift Ψ) is an idealised model. In reality, fish do not only adjust the phase of body undulations to interact with the flow nearby, and only tuning the body phase may result in limited energy savings. Future studies should consider more possible actions for fish swimming in turbulence with proprioceptive sensory feedback, such as frequency and amplitude, and explore other potential learning algorithms. Yet, our findings reveal how even a simple reinforcement learning algorithm can be powerful for optimising locomotion control in complex fluid environments.

Acknowledgments

LL acknowledges the Deutsche Forschungsgemeinschaft (DFG, German Research Foundation) under Germany's Excellence Strategy–EXC 2117-422037984, the Max Planck Society, and great support from the Couzin Lab. JD has been supported by the National Natural Science Foundation of China (Grant Nos. 11772299, 11922212). GX acknowledges the Natural Science Foundation of China (NSFC, Grant No. 61633002) and the Beijing Natural Science Foundation (Grant No. 4192026).

Data availability statement

The data that support the findings of this study are available upon reasonable request from the authors.

ORCID iDs

Liang Li https://orcid.org/0000-0002-2447-6295
Jian Deng https://orcid.org/0000-0001-6335-498X
Matthew J Lutz https://orcid.org/0000-0001-5944-2311
Guangming Xie https://orcid.org/0000-0001-6504-0087

References

[1] Vogel S 1996 *Life in Moving Fluids: The Physical Biology of Flow* (Princeton, NJ: Princeton University Press)
[2] Liao J C, Beal D N, Lauder G V and Triantafyllou M S 2003 The Karman gait: novel body kinematics of rainbow trout swimming in a vortex street *J. Exp. Biol.* **206** 1059–73
[3] Marras S, Killen S S, Lindström J, McKenzie D J, Steffensen J F and Domenici P 2014 Fish swimming in schools save energy regardless of their spatial position *Behav. Ecol. Sociobiol.* **69** 219–26
[4] Li L, Nagy M, Graving J M, Bak-Coleman J, Xie G and Couzin I D 2020 Vortex phase matching as a strategy for schooling in robots and in fish *Nat. Commun.* **11** 5408
[5] Rosenthal S B, Twomey C R, Hartnett A T, Wu H S and Couzin I D 2015 Revealing the hidden networks of interaction in mobile animal groups allows prediction of complex behavioral contagion *Proc. Natl Acad. Sci. USA* **112** 4690–5
[6] Coombs S, Bleckmann H, Fay R R and Popper A 2014 *The Lateral Line System* (Berlin: Springer)
[7] Liao J C 2006 The role of the lateral line and vision on body kinematics and hydrodynamic preference of rainbow trout in turbulent flow *J. Exp. Biol.* **209** 4077–90
[8] Gazzola M, Argentina M and Mahadevan L 2015 Gait and speed selection in slender inertial swimmers *Proc. Natl Acad. Sci. USA* **112** 3874–9
[9] Pollard B and Tallapragada P 2021 Learning hydrodynamic signatures through proprioceptive sensing by bioinspired swimmers *Bioinspir. Biomim.* **16** 026014
[10] Sherrington C S 1907 On the proprioceptive system, especially in its reflex aspect *Brain* **29** 467–82
[11] Proske U and Gandevia S C 2012 The proprioceptive senses: their roles in signaling body shape, body position and movement, and muscle force *Physiol. Rev.* **92** 1651–97
[12] Prochazka A 1996 Proprioceptive feedback and movement regulation *Handbook of Physiology, Exercise: Regulation and Integration of Multiple Systems* (Bethesda, MD: American Physiological Society) ch 3 pp 89–127
[13] Windhorst U 2007 Muscle proprioceptive feedback and spinal networks *Brain Res. Bull.* **73** 155–202
[14] Williams R, Neubarth N and Hale M E 2013 The function of fin rays as proprioceptive sensors in fish *Nat. Commun.* **4** 6
[15] Flammang B E and Lauder G V 2013 Pectoral fins aid in navigation of a complex environment by bluegill sunfish under sensory deprivation conditions *J. Exp. Biol.* **216** 3084–9
[16] Aiello B R, Hardy A R, Westneat M W and Hale M E 2018 Fins as mechanosensors for movement and touch-related behaviors *Integr. Comp. Biol.* **84** 2709
[17] Ijspeert A J 2008 Central pattern generators for locomotion control in animals and robots: a review *Neural Netw.* **21** 642–53
[18] Yu J, Tan M, Chen J and Zhang J 2013 A survey on CPG-inspired control models and system implementation *IEEE Trans. Neural Netw. Learn. Syst.* **25** 441–56
[19] Katz P S 2016 Evolution of central pattern generators and rhythmic behaviours *Phil. Trans. R. Soc.* B **371** 20150057
[20] Verma S, Novati G and Koumoutsakos P 2018 Efficient collective swimming by harnessing vortices through deep reinforcement learning *Proc. Natl Acad. Sci. USA* **115** 5849–54
[21] Kober J, Bagnell J A and Peters J 2013 Reinforcement learning in robotics: a survey *Int. J. Robot. Res.* **32** 1238–74
[22] Sutton R S and Barto A G 1998 *Reinforcement Learning: An Introduction* vol 1 (Cambridge, MA: MIT Press)
[23] Watkins C J C H and Dayan P 1992 Q-learning *Mach. Learn.* **8** 279–92
[24] Li L, Wang C and Xie G 2015 A general CPG network and its implementation on the microcontroller *Neurocomputing* **167** 299–305
[25] Li L, Wang C and Xie G 2014 Modeling of a carangiform-like robotic fish for both forward and backward swimming: based on the fixed point *Proc. IEEE Int. Conf. Robotics and Automation* pp 800–5
[26] Jasak H 1996 Error analysis and estimation in the finite volume method with applications of fluid flows *PhD Thesis* Imperial College, University of London
[27] Peskin C S 2002 The immersed boundary method *Acta Numer.* **11** 479–517
[28] Deng J, Mao X and Xie F 2019 Dynamics of flow around a circular cylinder with flexible filaments attached *Phys. Rev.* E **100** 053107
[29] Deng J, Mao X and Brandt L 2021 Symmetry breaking of tail-clamped filaments in Stokes flow *Phys. Rev. Lett.* **126** 124501
[30] Li L, Lv J, Chen W, Wang W, Zhang X and Xie G 2016 Application of Taguchi method in the optimization of swimming capability for robotic fish *Int. J. Adv. Robot. Syst.* **13** 102
[31] Zhu Y, Yuan H and Lee C 2015 Experimental investigations of the initial growth of flow asymmetries over a slender body of revolution at high angles of attack *Phys. Fluids* **27** 13
[32] Aiello B R, Westneat M W and Hale M E 2017 Mechanosensation is evolutionarily tuned to locomotor mechanics *Proc. Natl Acad. Sci. USA* **114** 4459–64
[33] Ristroph L, Liao J C and Zhang J 2015 Lateral line layout correlates with the differential hydrodynamic pressure on swimming fish *Phys. Rev. Lett.* **114** 018102
[34] Weihs D 1973 Hydromechanics of fish schooling *Nature* **241** 290–1